

Synthesis of pure phase BiFeO₃ powders by direct thermal decomposition of metal nitrates

Lei Wang^{a,b}, Jin-Bao Xu^{a,*}, Bo Gao^a, Liang Bian^a, Xue-Ying Chen^{a,b}

^a*Xinjiang Key Laboratory of Electronic Information Materials and Devices, Xinjiang Technical Institute of Physics & Chemistry, Chinese Academy of Sciences, 830011 Urumqi, China*

^b*Graduate University of Chinese Academy of Sciences, 100049 Beijing, China*

Available online 16 October 2012

Abstract

Pure phase BiFeO₃ powders were successfully synthesized by direct thermal decomposition of metal nitrates at 500 °C. The as-prepared BiFeO₃ had a perovskite structure which was studied using X-ray diffraction. The porous structures were investigated through scanning electron microscopy. Morphology of BiFeO₃ changed from micron-sized porous structures to nano-sized particles as NH₃HCO₃ was added. Furthermore, the mechanism of formation of BiFeO₃ was also discussed through X-ray diffraction, thermogravimetry and differential scanning calorimetry. The optical absorption band gap of the micro-sized porous structure BiFeO₃ is 1.8 eV.

© 2012 Elsevier Ltd and Techna Group S.r.l. All rights reserved.

Keywords: C. Magnetic properties; C. Optical properties; D. Ferrites

1. Introduction

BiFeO₃ is one of the most widely studied multiferroic materials with relatively high Neel temperature ($T_N=370^\circ\text{C}$) and Curie temperature ($T_C=830^\circ\text{C}$) [1]. It is well known that BiFeO₃ nanostructures exhibit unique electrical, magnetic and optical properties which are different from those of bulk samples due to their low dimensionality and quantum confinement effects [2]. Various methods have been developed for the preparation of micrometer- and nanometer-sized BiFeO₃ crystallites with different morphologies, such as hydrothermal synthesis [3–5], coprecipitation [6], sol–gel process [7], sonochemical and microemulsion techniques [8], combustion synthesis [9], mechanochemical synthesis [10] and other routes [11–14]. Each of these methods has its own advantages and limitations. It is still worth developing simpler, energy efficient and environmentally benign procedures to obtain BiFeO₃ micro/nano-powder with special morphologies and high purity.

The solid-state thermal decomposition of metal nitrates is one of the simplest and lowest-cost techniques for preparing pure and nanosized metal oxides with relatively high specific surface area at low temperature [15–17]. This technique not only avoided the need for a template and complex apparatus but also exhibited a capacity to control the shape of the target products. Inspired by this, we developed the direct thermal decomposition of metal nitrates procedure to prepare the micron-sized porous structure and nano-sized particle structure BiFeO₃ with different optical and magnetic behavior. Compared with other methods, this method exhibits many advantages in synthesis of special morphologies BiFeO₃: no need for solvent, surfactant and complex apparatus, high yield, low energy consumption and simple reaction technology.

2. Experimental procedure

In order to reduce the amount of Bi₂Fe₄O₉ and obtain homogeneous mixture, 1.05 mmol Bi(NO₃)₃·5H₂O (≥99%, Aladdin chemistry Co. Ltd.) and 1 mmol Fe(NO₃)₃·9H₂O (≥98.5%, Aladdin chemistry Co. Ltd.) were mixed in an agate mortar and ground with a pestle for 10 min. In order to

*Corresponding author. Tel./fax: +86 991 3835096.

E-mail address: xujb@ms.xjb.ac.cn (J.-B. Xu).

prepare BiFeO₃ nanoparticles, 10 mmol NH₄HCO₃ ($\geq 99\%$, Aladdin chemistry Co. Ltd.) (only in one sample) were added and ground for another 10 min. The mixture was calcined at 450–600 °C for 2 h in ambient air. The temperatures for the decomposition of the mixture were selected from the results of the TGA–DSC analysis. The decomposition products were leached with 20% HNO₃ to remove the unreacted Bi₂O₃ and then washed by deionized water for several times and dried at 80 °C for 3 h. The five samples obtained in this process are hereafter named S1 (calcined at 450 °C), S2 (calcined at 500 °C), S3 (calcined at 550 °C), S4 (calcined at 600 °C) and S5 (calcined at 500 °C, with NH₃HCO₃ added).

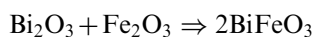
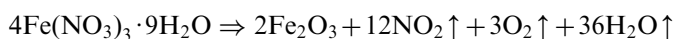
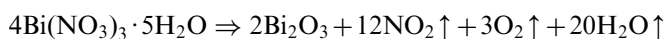
Powder X-ray diffraction (XRD, D8, Bruker, Germany) using Cu K α radiation ($\lambda = 1.54056 \text{ \AA}$) was adopted to identify the crystalline phase of the resulting materials. Thermal analysis was performed by thermogravimetric analysis and differential scanning calorimetry (TGA/DSC, STA 409, NETZSCH, Germany) at a heating rate of 10 °C/min in air. The grain size and morphology of BiFeO₃ were observed using scanning electron microscope (SEM, 1430VP, LEO, Germany). A vibrating-sample magnetometer (VSM, Lake Shore 7404, Lake Shore Cryotronics, Inc., USA) was used to study the magnetic properties of the prepared samples. The optical property was measured with an ultraviolet–visible spectrophotometer (UV–vis, U-3900 H, Hitachi, Japan).

3. Results and discussion

Fig. 1 shows the X-ray diffraction patterns of the samples. The sample calcined at 450 °C (S1) with no characteristic diffraction peaks indicating its amorphous structure. The samples calcined from 500 to 550 °C (S2, S3 and S5) shared similar diffraction patterns with no noticeable peaks from impurity phase detected. According to the JCPDS powder data (Card no. 20-0169), the BiFeO₃ powder has a perovskite structure. In the sample calcined at 600 °C (S4), impurity phase of Bi₂Fe₄O₉ was detected in

the major BiFeO₃ phase. Compared with the conventional solid-state reaction process ($\sim 800 \text{ °C}$) [18,19], the direct thermal decomposition of metal nitrates method can effectively lower the crystallization temperature of BiFeO₃ by about 300 °C.

Fig. 2 shows the TG–DSC curves of the metal nitrates (raw materials of S1, S2, S3 or S4). The endothermic peak in the DSC curve around 100.8 °C, accompanied by a relatively weight loss (8.8%) in the TG curve, may be due to the loss of absorbed water and water of crystallization. The endothermic peak around 146.9 °C and 169.4 °C is indicative of melting and decomposition of nitrates respectively. It can be seen that the weight loss of the raw materials started at 40 °C and continued till 500 °C, where weight loss almost stopped. XRD patterns show that pure BiFeO₃ has already formed at 500 °C, which is in good agreement with TG result. The exothermic peak around 729.2 °C may be due to the crystallization of Bi₂Fe₄O₉. The final mass percentage was around 43.5% after being heated up to 1100 °C. The relative weight loss (56.5%) in the TG curve may be attributed to H₂O, NO₂ and O₂ emission from decomposition of nitrates. The thermal decomposition of Bi(NO₃)₃·5H₂O, Fe(NO₃)₃·9H₂O and obtained BiFeO₃ could be formally presented as



Scanning electron microscopy (SEM) is performed to characterize the morphology and uniformity of all BiFeO₃ samples. Fig. 3a shows that S1 has a noticeable porous-like structure with nanoparticle regularity agglomeration. Fig. 3b and c show that S3 and S4 are composed of irregular particles. Compared with S2, it can be predicted that over-calcination may destroy the pore structure. As shown in Fig. 3d (S5), spherical nanoparticles with the average particle size of about 80–100 nm can be recognized.

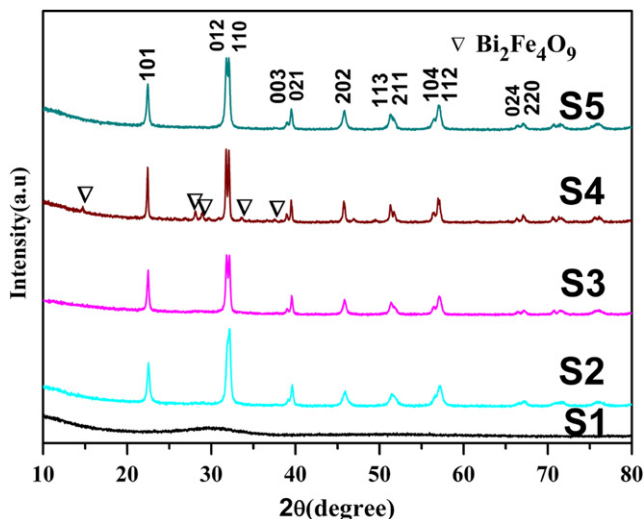


Fig. 1. XRD patterns of BiFeO₃ samples: S1, S2, S3, S4 and S5.

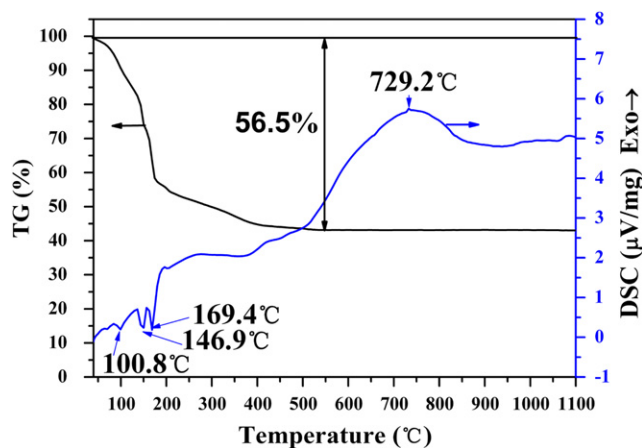


Fig. 2. TG/DSC curve of the metal nitrates (raw materials of S1, S2, S3 or S4).

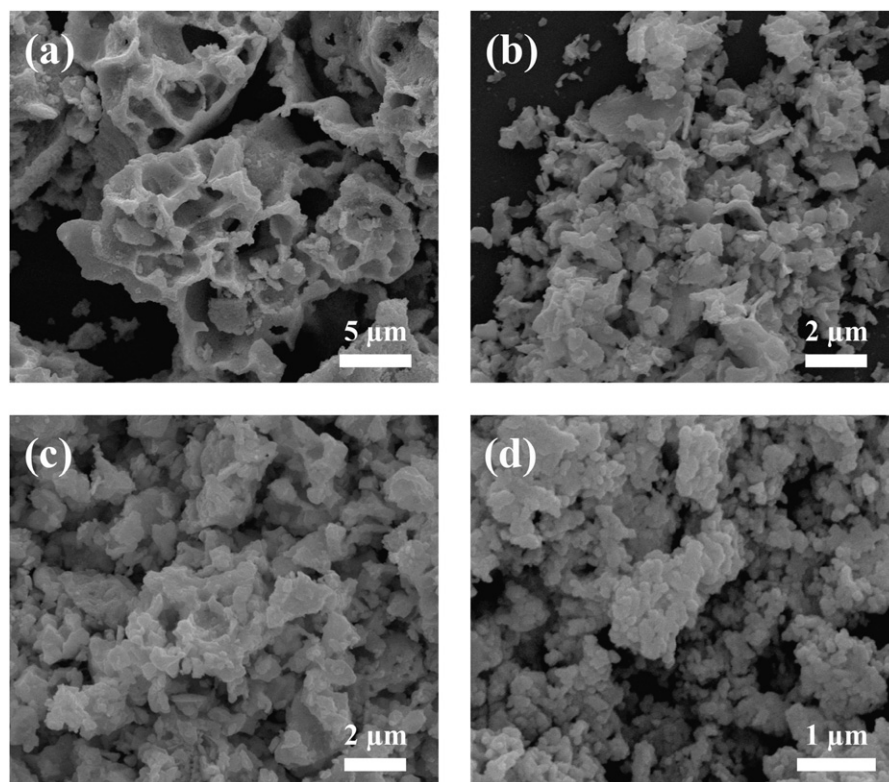


Fig. 3. SEM micrographs of (a) S2 (b) S3 (c) S4 and (d) S5.

The BiFeO_3 morphology changes from micron-sized porous structure to nano-particle structure as NH_3HCO_3 was added.

The possible formation mechanism of porous-like structure BiFeO_3 may be as follows: metal nitrates melt to liquid phase at first, then decompose to release gas phase. The porous structure is formed when the dispersed gas phase (discontinuous phase) is removed from the continuous phase of liquid. But the fabricated foams have low kinetic stability because of the large difference between the densities of the gas and liquid. The liquid phase tends to drain downwards while the gas tends to move upwards. As the calcine temperature increases from 500°C to 550°C (or 600°C), rate of gas production will increase rapidly, which breaks the formation of foam. When NH_4HCO_3 was added in metal nitrates mixture and calcined at the same temperature (500°C), spherical nanoparticle structure instead of porous-like structure BiFeO_3 was obtained. This can be attributed to the fast generation of additional inert gas by NH_4HCO_3 , which has the similar effect with that of temperature increase.

Fig. 4a shows the magnetization curve of the four BiFeO_3 samples measured at room temperature. The magnetic hysteresis loop of the sample S3, S4 and S5 shows linear field dependence. The $M-H$ curves of S2 present a noteworthy hysteresis loop. A partly enlarged curve of S2 is shown in Fig. 4b. The curve shows weak ferromagnetism at room temperature with a remanent magnetization value (M_r) of approximately 10 memu/g and a coercive field value (H_c) of nearly 55 Oe. It is well known that the wavelength of the incommensurate cycloid spin structure in bulk BiFeO_3 is 62 nm [20]. The cycloid

structure in bulk BiFeO_3 is partially destroyed in the BiFeO_3 nanostructures, which leads to the weak ferromagnetic behaviors at room temperature. Zou et al. [21] propose that different morphological BiFeO_3 own different magnetic properties. The properties and functions of chemical materials depend on the array of molecular components as well as the component itself. Our experimental results indicate that, compared with irregularity nanoparticles, the porous-like structure presents better magnetic property.

BiFeO_3 is a narrow bandgap metal oxide semiconductor useful for visible light active photocatalysis. The UV–vis absorption spectra of the samples are shown in Fig. 5a. We calculate the band gap from the plot of the Kubelka–Munk function $((ah\nu)^2)$ vs photon energy ($h\nu$) for direct band gap semiconductors, as presented in Fig. 5b. The optical bandgaps of the samples are estimated to be 1.8 eV (S2), 1.95 eV (S3), 2.01 eV (S4) and 2.14 eV (S5), which are smaller than the reported value of about 2.2–2.8 eV for bulk BiFeO_3 [22,23]. The results suggest that porous-like structure BiFeO_3 may have a wider application to photocatalyst and optoelectric devices, especially under the visible light wave band.

4. Conclusions

In summary, micron-sized porous structure and nano-sized particle structure BiFeO_3 samples were successfully synthesized through direct thermal decomposition of metal nitrates at 500°C . The optical absorption band gap of the

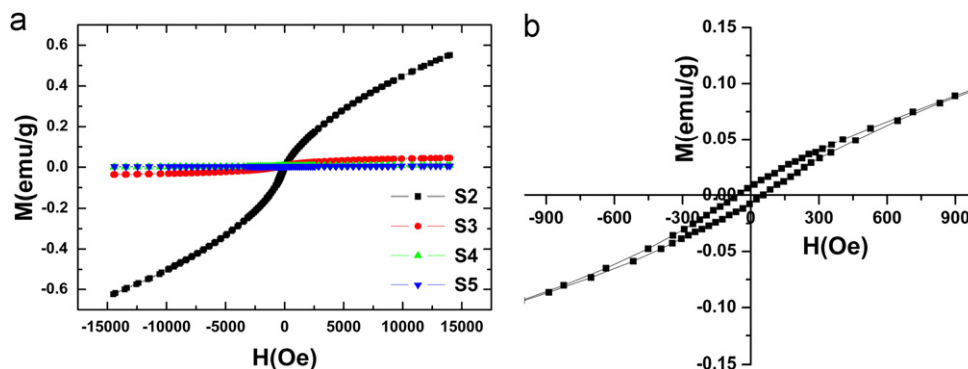


Fig. 4. (a) VSM measurement of different BiFeO₃ particles synthesized from 500 to 600 °C, and (b) the partially enlarged curve of BiFeO₃ sample S2.

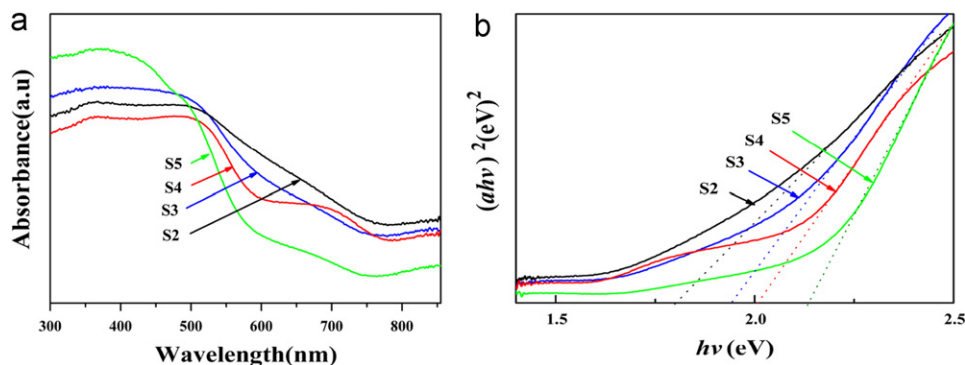


Fig. 5. (a) UV–vis absorption spectra of different BiFeO₃ samples, and (b) calculated band gaps of BiFeO₃ samples with the tangent of the linear part as dotted line.

micron-sized porous structure BiFeO₃ is 1.8 eV, which is smaller than that of bulks or thin films. Uniform and spherical BiFeO₃ nanoparticles, with the band gap of 2.14 eV, can also be obtained by this method (with NH₃HCO₃ added). The method is simple, low-cost, safe and suitable for industrial production of high purity BiFeO₃ with special morphologies for various applications.

Acknowledgments

This work was financially supported by the Youth Science Foundation of Xinjiang Uygur Autonomous Region of China (Grant no. 2011211B49), the One Hundred Talents Project Foundation Program and the Western Light Talent Culture Project (Grant no. Y12S311301) of Chinese Academy of Sciences.

References

- [1] J. Wang, J.B. Neaton, H. Zheng, V. Nagarajan, S.B. Ogale, B. Liu, D. Viehland, V. Vaithyanathan, D.G. Schlom, U.V. Waghmare, N.A. Spaldin, K.M. Rabe, M. Wuttig, R. Ramesh, Epitaxial BiFeO₃ multiferroic thin film heterostructures, *Science* 299 (2003) 1719–1722.
- [2] F. Gao, X.Y. Chen, K.B. Yin, S. Dong, Z.F. Ren, F. Yuan, T. Yu, Z. Zou, J.M. Liu, Visible-light photocatalytic properties of weak magnetic BiFeO₃ nanoparticles, *Advanced Materials* 19 (19) (2007) 2889–2892.
- [3] C. Chen, J.R. Cheng, S.W. Yu, L.J. Che, Z.Y. Meng, Hydrothermal synthesis of perovskite bismuth ferrite crystallites, *Journal of Crystal Growth* 291 (1) (2006) 135–139.
- [4] S. Basu, M. Pal, D. Chakravorty, Magnetic properties of hydrothermally synthesized BiFeO₃ nanoparticles, *Journal of Magnetism and Magnetic Materials* 320 (24) (2008) 3361–3365.
- [5] Y.G. Wang, G. Xu, Z.H. Ren, X. Wei, W.J. Weng, P. Du, G. Shen, G.R. Han, Mineralizer-assisted hydrothermal synthesis and characterization of BiFeO₃ nanoparticles, *Journal of the American Ceramic Society* 90 (8) (2007) 2615–2617.
- [6] S. Shetty, V. Palkar, R. Pinto, Size effect study in magnetoelectric BiFeO₃ system, *Pramana Journal of Physics* 58 (5-6) (2002) 1027–1030.
- [7] T. Liu, Y.B. Xu, J.Y. Zhao, Low-temperature synthesis of BiFeO₃ via PVA sol–gel route, *Journal of the American Ceramic Society* 93 (11) (2010) 3637–3641.
- [8] N. Das, R. Majumdar, A. Sen, H.S. Maiti, Nanosized bismuth ferrite powder prepared through sonochemical and microemulsion techniques, *Materials Letters* 61 (10) (2007) 2100–2104.
- [9] S. Farhadi, M. Zaidi, Bismuth ferrite (BiFeO₃) nanopowder prepared by sucrose-assisted combustion method: a novel and reusable heterogeneous catalyst for acetylation of amines, alcohols and phenols under solvent-free conditions, *Journal of Molecular Catalysis A: Chemical* 299 (1-2) (2009) 18–25.
- [10] I. Szafraniak, M. Polomska, B. Hilczer, A. Pietraszko, L. Kepinski, Characterization of BiFeO₃ nanopowder obtained by mechanochemical synthesis, *Journal of the European Ceramic Society* 27 (13–15) (2007) 4399–4402.
- [11] Y. Hu, L. Fei, Y. Zhang, J. Yuan, Y. Wang, H. Gu, Synthesis of bismuth ferrite nanoparticles via a wet chemical route at low temperature, *Journal of Nanomaterials* 2011 (2011) 1–6.
- [12] T. Xian, H. Yang, X. Shen, J.L. Jiang, Z.Q. Wei, W.J. Feng, Preparation of high-quality BiFeO₃ nanopowders via a polyacrylamide gel route, *Journal of Alloys and Compounds* 480 (2) (2009) 889–892.

- [13] X.B. He, L.A. Gao, Synthesis of pure phase BiFeO_3 powders in molten alkali metal nitrates, *Ceramics International* 35 (3) (2009) 975–978.
- [14] S. Ghosh, S. Dasgupta, A. Sen, H.S. Maiti, Low temperature synthesis of bismuth ferrite nanoparticles by a ferrioxalate precursor method, *Materials Research Bulletin* 40 (12) (2005) 2073–2079.
- [15] S. Farhadi, J. Safabakhsh, Solid-state thermal decomposition of the $[\text{Co}(\text{NH}_3)_5\text{CO}_3]\text{NO}_3 \cdot 0.5\text{H}_2\text{O}$ complex: a simple, rapid and low-temperature synthetic route to Co_3O_4 nanoparticles, *Journal of Alloys and Compounds* 515 (2012) 180–185.
- [16] S. Farhadi, Z. Roostaei-Zaniyani, Preparation and characterization of NiO nanoparticles from thermal decomposition of the $[\text{Ni}(\text{en})_3](\text{NO}_3)_2$ complex: a facile and low-temperature route, *Polyhedron* 30 (6) (2011) 971–975.
- [17] A. Pathak, S. Mohapatra, S. Mohapatra, S.K. Biswas, D. Dhak, N.K. Pramanik, A. Tarafdar, P. Pramanik, Preparation of nanosized mixed-oxide powders, *American Ceramic Society Bulletin* 83 (2004) 9301–9306.
- [18] Y.P. Wang, L. Zhou, M.F. Zhang, X.Y. Chen, J.M. Liu, Z.G. Liu, Room-temperature saturated ferroelectric polarization in BiFeO_3 ceramics synthesized by rapid liquid phase sintering, *Applied Physics Letters* 84 (10) (2004) 1731–1733.
- [19] S.M. Selbach, M.A. Einarsrud, T. Grande, On the thermodynamic stability of BiFeO_3 , *Chemistry of Materials* 21 (2009) 169–173.
- [20] D. Lebeugle, D. Colson, A. Forget, M. Viret, A.M. Bataille, A. Gukasov, Electric-field-induced spin flop in BiFeO_3 single crystals at room temperature, *Physical Review Letters* 100 (2008) 227602.
- [21] J. Zou, J.Z. Jiang, Y.X. Zhang, J.N. Ma, Q.J. Wan, A comparative study of the optical, magnetic and electrocatalytic properties of nano BiFeO_3 with different morphologies, *Materials Letters* 72 (2012) 134–136.
- [22] L. Fei, J. Yuan, Y. Hu, C. Wu, J. Wang, Y. Wang, Visible light responsive perovskite BiFeO_3 pills and rods with dominant $\{111\}$ facets, *Crystal Growth and Design* 11 (4) (2011) 1049–1053.
- [23] P. Chen, N.J. Podraza, X.S. Xu, A. Melville, E. Vlahos, V. Gopalan, R. Ramesh, D.G. Schlom, J.L. Musfeldt, Optical properties of quasi-tetragonal BiFeO_3 thin films, *Applied Physics Letters* 96 (2010) 131907.